Recent Developments in Electronics and Communication Systems
KVS Ramachandra Murthy et al. (Eds.)

doi:10.3233/ATDE221244

Analysis of Kinematics of a 12-DOF Biped Robot Gait by Parametrization of Its Body Trajectories

Aarti Chauhan[a,1] and Jitendra Kumar[b]
[a]*Centre For Advance Studies, Lucknow*
[b]*Centre For Advance Studies, Lucknow*

Abstract. This paper focuses on modeling forward and inverse kinematics of a 12-DOF bipedal robot and parametrizing its body trajectory to generate different gaits on 3D terrain.The 12-DOF kinematic chain represents the lower body part of the humanoid robot. The Cartesian coordinate is assigned to each link of the biped robot using the Denavit-Hartenberg (DH) convention. One step of the bipedal walk is divided into three walk phases depending on whether one foot or both feet are in contact with the ground.Time parameterized cubic splines construct the biped robot's mid-hip and swinging foot trajectory.The inverse kinematic determines the values of the joint angles corresponding to hip and swinging foot frame trajectory using the geometric relation between foot ankle point, knee position,and hip position. The complete one-step gait of the biped robot is represented in the form of a stick diagram.The proposed method is a geometrical approach to parameterize the gait of a biped robot for one step of the walk in terms of hip and swinging foot trajectory optimization is required to determine energy optimal balanced gait, which we envisage as our future task.

Keywords. Biped Robot, Gait Synthesis, Body Trajectory parameterization.

1. Introduction

In recent decades research on mobile robots has gained attention. Mobile robots can be classified based on whether they use legs, wheels, or tracks to navigate from one place to another. The Biped robot movement has attracted much interest in recent years. Biped robot has the potential for human-like movement, especially when navigating uneven ground, steep stairs, and congested areas.A biped robot is the humanoid robot's lower body part (two legs and a hip).Biped robots having different DOF, such as 4-DOF,8-DOF, and 12-DOF, have been studied.This paper presents systematic kinematic modeling of a 12-DOF of a biped robot by parametrizing its body trajectories. This paper explains the kinematic complexity of the biped robot by a detailed discussion of forward and inverse kinematics and determining the inverse kinematic solution of the joint angles using the geometrical method. The relation between a biped robot's left and right gait has been discussed in [1] ; authors have explained a method of generating an efficient and faster optimal gait on uneven terrain for a 14-DOF biped robot using the dynamic

[1] Aarti Chauhan, Centre For Advanced Studies, Lucknow,226031; E-mail:chauhanaarti60@gmail.com.

similarity principle of gaits.Vukobratovic et al.[2], [3] proposed the concept of zero moment point (ZMP), a stability criterion that ensures balancing during walking. They defined ZMP as the location on the ground where the moment of all gravitational and inertial forces acting on the robot is zero around two axes situated on the ground's plane.

They suggested that keeping this point within a supporting polygon during motion is a sufficient criterion for stability. C. Hernández-Santos et al.[4] proposed a new biped robot structure with seven DOF of each leg with 1- DOF related to the toe joint and also presented the approximate equations for kinematics by using the sagittal and frontal planes to divide the walking gait. They have used SimMechanics of MATLAB toolbox and Solid Works for simulation and numerical examples to prove the analytical results.The Principle of Lagrangian dynamics concepts is used to control the desired trajectories and determine the torque the joints need, which applies a PD control law with gravity compensation. Huang et al.[5] suggested a method for synthesizing gaits without previously defining the ideal ZMP trajectory. This technique uses cubic spline interpolation to plan the foot and hip trajectory in cartesian space.The iterative calculation was used to generate the two parameters that were used to design the smooth hip motion to maximize the stability margin. The representation of the biped stride typically leads to descriptions of the kinematics, dynamics, and stability of two-legged walking robots.This problem remains unsolved because most methods minimize the dynamic model of the humanoid robot to an inverted pendulum based on either a straightforward observation or a mathematical analysis derived from kinematics [6]. Chevallereau and Aoustin [7] achieved optimal cyclic stride for a bipedal robot.They assumed the joint variables were polynomial functions and subsequently found their coefficients to maximize walking speed. Dip et al.[8] enhanced the bipedal stride by considering balanced margin and speed.They used a genetic algorithm (GA) to enhance the stability margin by optimizing the critical walking trajectory and step length parameters for a given step period. Tlalolini et al. [9] attempted to create a path that would reduce a biped's energy expenditure while allowing for the necessary speed. They then attempted to speed up their walking using a search approach that gradually raised the intended pace. The purpose of studying this paper,which produces a workable combination of stepping frequency and length of an assumed biped,is to understand the impact of changes in two fundamental walking parameters,stepping frequency and length, on maximum speed and used energy. A new approach for creating the best gait possible using GA was suggested by Capi et al. [10], and ZMP requirements were considered an objective function restriction. The ability of bipeds to move instantly improved during their evolution. The forward model is traditionally constructed using a set of geometric transformations; however, it can also be created using a simplified method such as the Denavit - Hartenberg Method [11]. Kumagai et al. created a biped robot with seven degrees of freedom in each leg and a passive toe joint [12]. Neha and shuhaib [13], [14] has done the kinematic analysis and also planned the motion of the fingers such that ,The general solution of joint velocity was interpreted using the generalised inverse of the jacobian matrix; however, this work is accomplished using the pseudo-inverse of the jacobian matrix. E.Neha et al. [15] proposed the redundancy resolution schema that was applied to four finger tendon actuated robotic hand and observed that schema can solve redundancies of any robotic hand. Our proposed method provides a generalized framework for generating different gaits by varying the body trajectory parameters. This can be used to synthesis and kinematic analysis of biped robot gait on different types of terrain

This paper is organized as follows. The second section represents the model of a 12-DOF bipedal robot and also discusses DH-parameter.Section 3 explains the method to determine the Forward Kinematic of the biped Robot using the Denavit-Hartenberg convention.The inverse kinematic present in the sagittal planes is discussed in section 4.In Section 5,gait generation by parametrization of body trajectories of biped robots has been described.The results and discussion is presented in section 6.The last Section-7 represents several important conclusion and future work.

2. Model of the 12-DOF Biped Robot

This paper discusses the kinematics, dynamics, and body trajectory parametrization of a 12-DOF (12 revolute joint) Biped robot. It consists of two 6- DOF legs;each has a 2 DOF ankle, a 1-DOF knee, and a 3-DOF hip, as shown in Fig. 1.In recent years many biped robot models have been studied $\{\mathbf{x}_i, \mathbf{y}_i, \mathbf{z}_i\}$ denotes the coordinate system attached to ith link and θ_i represent the angle between $\mathbf{x}_{i-1}$ and $\mathbf{x}_i$ about $\mathbf{z}_{i-1}$, for $i = 0,\ldots,12$.The Denavit -Hartenberg (DH) [11] convention is used to assign coordinate system $(\mathbf{x}_i, \mathbf{y}_i, \mathbf{z}_i)$ to each link of the biped robot.

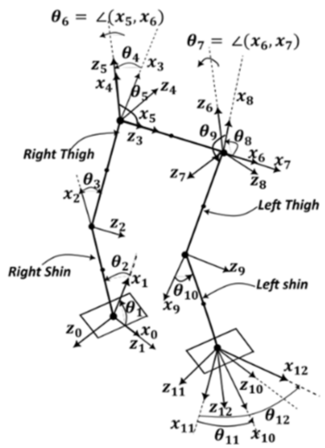

Figure 1: Model of a 12-DOF biped robot

S.No.	Frames	θ_i	d_i	α_i	a_i
1	0-1	θ_1	0	$\frac{\pi}{2}$	0
2	1-2	θ_2	0	0	l
3	2-3	θ_3	0	0	l
4	3-4	θ_4	0	$\frac{\pi}{2}$	0
5	4-5	θ_5	0	$\frac{\pi}{2}$	0
6	5-6	θ_6	0	0	l_h
7	6-7	θ_7	0	$\frac{\pi}{2}$	0
8	7-8	θ_8	0	$\frac{\pi}{2}$	0
9	8-9	θ_9	0	0	l
10	9-10	θ_{10}	0	0	l
11	10-11	θ_{11}	0	$\frac{\pi}{2}$	0
12	11-12	θ_{12}	0	$\frac{\pi}{2}$	0

Table 1 : DH-parameter Table

The Table 1 show the DH-parameters where, θ_i is the angle measured about the $\mathbf{z}_{i-1}$ axis between the $\mathbf{x}_{i-1}$ and $\mathbf{x}_i$ axis, d_i is the distance measured along the $\mathbf{z}_{i-1}$ axis from the origin of $(i-1)$th coordinate system to the point of intersection of $\mathbf{x}_i$ axis with $\mathbf{z}_{i-1}$ axis, α_i is the angle measured about the $\mathbf{x}_{i-1}$ axis between the $\mathbf{z}_{i-1}$ and $\mathbf{z}_i$ axis and a_i is the distance measured along the $\mathbf{x}_{i-1}$ axis from the intersection point of $\mathbf{x}_i$ with $\mathbf{z}_{i-1}$ to the origin of ith coordinate system.

3. Forward Kinematic of a 12-DOF Biped Robot

Forward kinematics [16] is used to determine the location and orientation of the end-effector from the configurations of the robot’s joint angle.The structures of a humanoid robot’s left leg are identical to the mirror image of the right leg;this paper uses the same coordinate frames for both legs for easy analysis.The forward Kinematic determines the position and orientation of the biped robot's swinging foot in the base reference frame.Table 1 Shows the coordinate system attached to the right and left leg links.DH-parameters a_i and d_i of both legs are fixed,and only parameters the θ_i change.The ransformation matrix of 12-DOF of a biped robot of each frame.The link transformation matrix of a 12-DOF biped robot is as follows:

$$T_1^0 = \begin{bmatrix} cos\theta_1 & 0 & sin\theta_1 & 0 \\ sin\theta_1 & 0 & -cos\theta_1 & 0 \\ 0 & 0 & 0 & 1 \\ 0 & 0 & 0 & 1 \end{bmatrix}, \boldsymbol{T}_2^1 = \begin{bmatrix} cos\theta_2 & -sin\theta_2 & 0 & lcos\theta_2 \\ sin\theta_2 & cos\theta_2 & 0 & lsin\theta_2 \\ 0 & 0 & 1 & 0 \\ 0 & 0 & 0 & 1 \end{bmatrix},$$
$$\boldsymbol{T}_3^2 = \begin{bmatrix} cos\theta_3 & -sin\theta_3 & 0 & lcos\theta_3 \\ sin\theta_3 & cos\theta_3 & 0 & lsin\theta_3 \\ 0 & 0 & 1 & 0 \\ 0 & 0 & 0 & 1 \end{bmatrix}, \boldsymbol{T}_4^3 = \begin{bmatrix} cos\theta_4 & 0 & sin\theta_4 & 0 \\ sin\theta_4 & 0 & -cos\theta_4 & 0 \\ 0 & 1 & 0 & 0 \\ 0 & 0 & 0 & 1 \end{bmatrix}, \quad (1)$$
$$\boldsymbol{T}_5^4 = \begin{bmatrix} cos\theta_5 & 0 & sin\theta_5 & 0 \\ sin\theta_5 & 0 & -cos\theta_5 & 0 \\ 0 & 1 & 0 & 0 \\ 0 & 0 & 0 & 1 \end{bmatrix}, \boldsymbol{T}_6^5 = \begin{bmatrix} cos\theta_6 & -sin\theta_6 & 0 & l_h cos\theta_6 \\ sin\theta_6 & cos\theta_6 & 0 & l_h sin\theta_6 \\ 0 & 0 & 1 & 0 \\ 0 & 0 & 0 & 1 \end{bmatrix}$$

$$\boldsymbol{T}_7^6 = \begin{bmatrix} cos\theta_7 & 0 & sin\theta_7 & 0 \\ sin\theta_7 & 0 & -cos\theta_7 & 0 \\ 0 & 1 & 0 & 0 \\ 0 & 0 & 0 & 1 \end{bmatrix}, \boldsymbol{T}_8^7 = \begin{bmatrix} cos\theta_8 & 0 & sin\theta_8 & 0 \\ sin\theta_8 & 0 & -cos\theta_8 & 0 \\ 0 & 1 & 0 & 0 \\ 0 & 0 & 0 & 1 \end{bmatrix},$$
$$\boldsymbol{T}_9^8 = \begin{bmatrix} cos\theta_9 & -sin\theta_9 & 0 & lcos\theta_9 \\ sin\theta_9 & cos\theta_9 & 0 & lsin\theta_9 \\ 0 & 0 & 1 & 0 \\ 0 & 0 & 0 & 1 \end{bmatrix}, \boldsymbol{T}_{10}^9 = \begin{bmatrix} cos\theta_{10} & -sin\theta_{10} & 0 & lcos\theta_{10} \\ sin\theta_{10} & cos\theta_{10} & 0 & lsin\theta_{10} \\ 0 & 0 & 1 & 0 \\ 0 & 0 & 0 & 1 \end{bmatrix}, \quad (2)$$
$$\boldsymbol{T}_{11}^{10} = \begin{bmatrix} cos\theta_{11} & 0 & sin\theta_{11} & 0 \\ sin\theta_{11} & 0 & -cos\theta_{11} & 0 \\ 0 & 1 & 0 & 0 \\ 0 & 0 & 0 & 1 \end{bmatrix}, \boldsymbol{T}_{12}^{11} = \begin{bmatrix} cos\theta_{12} & 0 & sin\theta_{12} & 0 \\ sin\theta_{12} & 0 & -cos\theta_{12} & 0 \\ 0 & 1 & 0 & 0 \\ 0 & 0 & 0 & 1 \end{bmatrix}$$

4. Inverse Kinematic of a 12-Dof Biped Robot Using the Geometric Method

This section describes the geometric method for solving inverse Kinematic problems. In an inverse kinematic, the joint variable (angles) in terms of hip and foot position and orientation is determined in the base frames of the support foot.In reference,[17],The derivation of closed-form equations for the inverse kinematics chains is found to be more difficult than for the forward kinematics in the literature. In Figure 2(a), point H represents the coordinate of the right hip in base frame $\{0\}$ as (h_x, h_y, h_z) and l is the length of the shin and the length of the thigh of both legs. Using the property of triangle OHK and law of cosine, joint angle (θ_2 and θ_3) are determined as:

$$\boldsymbol{x}_2 = \frac{\overrightarrow{OK}}{|\overrightarrow{OK}|}, \qquad \overrightarrow{KH} = (\overrightarrow{OH} - \overrightarrow{OK}) \quad (3)$$

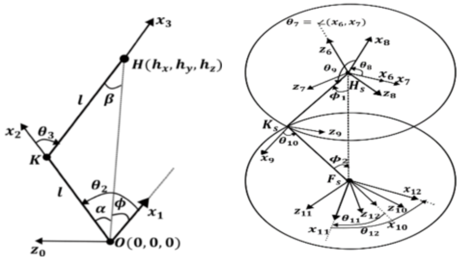

(a) (b)

Figure 2: (a) Inverse Kinematic of support leg, and (b) Inverse Kinematic of swinging leg

The cross product of $\overrightarrow{OH}$ vector and z_0 vector then the third resultant vector will comes out the perpendicular to the plane of the shin and thigh.

$$\boldsymbol{n}_\pi = \frac{\overrightarrow{OH} \times \boldsymbol{z}_0}{|\overrightarrow{OH} \times \boldsymbol{z}_0|} \tag{4}$$

where vector OH is formed by joining the support foot ankle point O with the origin of frame $\{5\}$, H as shown in Figure 2(a). The vector $\mathbf{n}_\pi$ is normal to plane formed by points O, K, and H.

$$\theta_1 = \pi/2 - \angle(\boldsymbol{n}_\pi, x_0) \tag{5}$$

$$\theta_2 = acos(x_1 \cdot x_2) \tag{6}$$

$$\widehat{KH} = \frac{\overrightarrow{KH}}{|\overrightarrow{KH}|}, \qquad \theta_3 = -acos(x_2 \cdot \widehat{KH}) \tag{7}$$

After finding the θ_1, θ_2 and θ_3 , the homogeneous transformation matrix $\boldsymbol{T}_6^3$ is computed as:

$$\boldsymbol{T}_6^3 = (\boldsymbol{T}_3^0)^{-1}\boldsymbol{T}_6^0 \tag{8}$$

$$\theta_5 = acos(-\boldsymbol{T}_6^3(3,3)) \tag{9}$$

$$\theta_4 = asin\left(\frac{\boldsymbol{T}_6^3(2,3)}{sin\theta_5}\right) \tag{10}$$

$$\theta_6 = asin\left(\frac{-\boldsymbol{T}_6^3(3,2)}{sin\theta_5}\right) \tag{11}$$

The inverse kinematics of the swinging leg is explained geometrically in Figure 2(b). The coordinate of the swinging foot is obtained by finding the intersection of two circles; the first circle has the center at the origin of reference frame-$\{6\}$ shown as point H_s with radius l. Second circle has center at the origin of reference frame-$\{12\}$ (point F_s) and radius l.The intersection point of circles is the knee of the swinging leg denoted by K_s. After obtaining the coordinate of swinging leg knee, the homogeneous transformation matrix $\boldsymbol{T}_9^6$ is obtained as:

$$\boldsymbol{T}_9^6 = (\boldsymbol{T}_6^0)^{-1}\boldsymbol{T}_9^0 \tag{12}$$

$$\theta_7 = asin\left(\frac{\boldsymbol{T}_9^6(2,3)}{sin\theta_8}\right) \tag{13}$$

$$\theta_8 = acos(-\boldsymbol{T}_9^6(3,3)) \quad (14)$$

$$\theta_9 = acos\left(\frac{\boldsymbol{T}_9^6(3,1)}{sin\theta_8}\right) \quad (15)$$

$$\phi_1 = acos\left(\frac{|\overrightarrow{H_sF_s}|}{2|H_sK_s|}\right), \quad \phi_2 = acos\left(\frac{|\overrightarrow{H_sF_s}|}{2|F_sK_s|}\right)$$
$$\theta_{10} = \phi_1 + \phi_2 \quad (16)$$

Where H_s,K_s, and F_s denotes the origin of reference frames-{6}, {9}, and {12} respectively. The homogeneous transformation matrix $\mathbf{T}_{12}^{10}$ is computed by multiplying inverse of $\boldsymbol{T}_{10}^0$ with $\boldsymbol{T}_{12}^0$.

$$\boldsymbol{T}_{12}^{10} = (\boldsymbol{T}_{10}^0)^{-1}\boldsymbol{T}_{12}^0 \quad (17)$$

$$\theta_{11} = acos(-\boldsymbol{T}_{12}^{10}(3,3)) \quad (18)$$

$$\theta_{12} = asin(\boldsymbol{T}_{12}^{10}(1,2)) \quad (19)$$

5. Gait Generation of the Biped Robot by Varying Parameterized Body Trajectories Variables

One-step walk of the biped robot is divided into three distinct phases:The first double support phase ($dsp1$) lies between initial time t_0 and double support-1 time t_{dsp1}.The single support phase (ssp) lies between double support-1 time $t_{dsp1}$and double support-2 ($dsp2$) time t_{dsp2}. Mid-duration of gait is specified by time t_m.The second double support phase lies between start of $dsp2$ time t_{dsp2}, and end of $dsp2$ time t_f.

5.1. Cubic spline based hip trajectory

Reference frame {6} represents the hip of the biped robot. Hip trajectory means variation in position and orientation of hip (reference frame-{6}) during the gait. The x_{hip},y_{hip}, z_{hip} and θ_{hip} coordinates of the hip are constructed by a cubic polynomial that satisfies the following conditions:

$$t_{knot\ \ hip} = [t_0, \ \ t_{dsp1}, \ \ t_m, \ \ t_{dsp2}, \ \ t_f] \quad (20)$$

$$X_{knot\ \ hip} = [x_{hip}(t_0), \ \ x_{hip}(t_{dsp1}), \ \ x_{hip}(t_m), \ \ x_{hip}(t_{dsp2}), \ \ x_{hip}(t_f)] \quad (21)$$

$$Y_{knot\ \ hip} = [y_{hip}(t_0), \ \ y_{hip}(t_{dsp1}), \ \ y_{hip}(t_m), \ \ y_{hip}(t_{dsp2}), \ \ y_{hip}(t_f)] \quad (22)$$

$$Z_{knot\ \ hip} = [z_{hip}(t_0), \ \ z_{hip}(t_{dsp1}), \ \ z_{hip}(t_m), \ \ z_{hip}(t_{dsp2}), \ \ z_{hip}(t_f)] \quad (23)$$

The rotation of the hip about $\mathbf{y}_0$ axis is defined by angle $\theta_{hip}(t)$. The variation of hip angle during the walk is defined by cubic splines satisfying the following condition:

$$\theta_{knot\ \ hip} = [\theta_{hip}(t_0), \ \ \theta_{hip}(t_{dsp1}), \ \ \theta_{hip}(t_m), \ \ \theta_{hip}(t_{dsp2}), \ \ \theta_{hip}(t_f)] \quad (24)$$

Using the hip coordinate and hip-angle trajectories, the homogeneous transformation matrix $\boldsymbol{T}_0^6(t)$ is defined at each instant during gait.

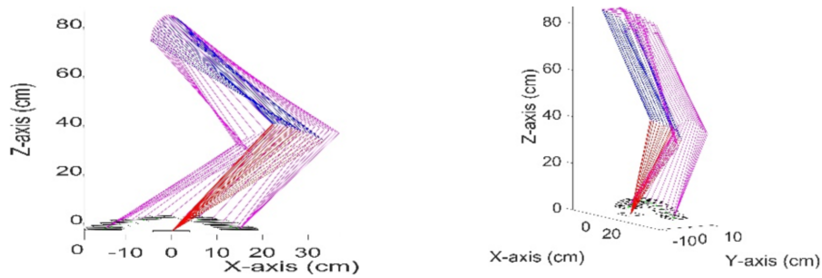

(a) (b)

Figure 3: Biped Robot Stick Diagram: (a) Side View, (b) 3D -View

5.2. Cubic spline based foot trajectory

Reference frame $\{12\}$ represents the swinging foot of the biped robot. Foot trajectory means variation in position and orientation of the foot during the gait.The x_{foot},y_{foot},z_{foot} are coordinates of the swinging foot ankle point constructed by a cubic polynomial that satisfies the following constraints:

$$t_{knot\ \ foot} = [t_0,\ \ t_{dsp1},\ \ t_m,\ \ t_{dsp2},\ \ t_f] \tag{25}$$

$$X_{knot\ \ foot} = [x_{foot}(t_0),\ \ x_{foot}(t_{dsp1}),\ \ x_{foot}(t_m),\ \ x_{foot}(t_{dsp2}),\ \ x_{foot}(t_f)] \tag{26}$$

$$Y_{knot\ \ foot} = [y_{foot}(t_0),\ \ y_{foot}(t_{dsp1}),\ \ y_{foot}(t_m),\ \ y_{foot}(t_{dsp2}),\ \ y_{foot}(t_f)] \tag{27}$$

$$Z_{knot\ \ foot} = [z_{foot}(t_0),\ \ z_{foot}(t_{dsp1}),\ \ z_{foot}(t_m),\ \ z_{foot}(t_{dsp2}),\ \ z_{foot}(t_f)] \tag{28}$$

The rotation matrix of frame-$\{12\}$ is defined by three Euler angles $\theta_{foot}(t), \phi_{foot}(t), \psi_{foot}(t)$. Cubic splines define the variation of the Euler's angle during the walk.Using the foot angle coordinates and Euler's-angles, the homogeneous transformation matrix $\mathbf{T}_{12}^{0}(t)$ is formed at each instant during gait.

6. Results and Discussion

A biped robot's initial and final configuration defines a one-step gait on uneven terrain. Therefore the position and orientation of reference frame $\{6\}, \boldsymbol{T}_6^0(t_0)$ and reference frame $\{12\}, \boldsymbol{T}_{12}^0(t_0)$ fixes the initial and final configuration of one step gait. By putting different values in $X_{knot\,foot}$,$Y_{knot\,foot}$,$Z_{knot\ \ foot}$ and $X_{knot\ \ hip}$,$Y_{knot\ \ hip}$,$Z_{knot\,hip}$, $\theta_{knot\ \ hip}$ and orientation of swinging foot diverse bipedal gaits can be generated. An example of bipedal gait for walking on flat ground with specified step length in form of stick diagram is shown in Figure 3.The joints angle variation and hip and foot trajectories are shown in figures 4, respectively.The initial and final position and orientation of hip (reference frame-$\{6\}$) and foot (reference frame-$\{12\}$) for generating this type of gait is:

$$\overbrace{\boldsymbol{T}_6^0(t_0) = \begin{bmatrix} 1 & 0 & 0 & 8 \\ 0 & 0 & 1 & 70 \\ 0 & -1 & 0 & -4 \\ 0 & 0 & 0 & 1 \end{bmatrix}}^{Configuration\ of\ hip\ at\ initial\ time}, \quad \overbrace{\boldsymbol{T}_6^0(t_f) = \begin{bmatrix} 1 & 0 & 0 & 8 \\ 0 & 0 & 1 & 70 \\ 0 & -1 & 0 & 4 \\ 0 & 0 & 0 & 1 \end{bmatrix}}^{Configuration\ of\ hip\ at\ endtime}$$
$$\overbrace{\boldsymbol{T}_{12}^0(t_0) = \begin{bmatrix} 1 & 0 & 0 & 8 \\ 0 & 0 & -1 & 0 \\ 0 & 1 & 0 & -15 \\ 0 & 0 & 0 & 1 \end{bmatrix}}^{Configuration\ of\ swinging\ foot\ at\ initial\ time}, \quad \overbrace{\boldsymbol{T}_{12}^0(t_f) = \begin{bmatrix} 1 & 0 & 0 & 8 \\ 0 & 0 & -1 & 0 \\ 0 & 1 & 0 & 15 \\ 0 & 0 & 0 & 1 \end{bmatrix}}^{Configuration\ of\ swinging\ time\ at\ the\ endtime} \tag{29}$$

Different bipedal gaits such as walking on flat, inclined, or uneven ground with varying step lengths, step height, and lateral displacement of swinging foot can be generated by changing the homogeneous transformation matrices $\mathbf{T}_6^0(t_0)$, $\mathbf{T}_6^0(t_f)$, $\mathbf{T}_{12}^0(t_0)$, and $\mathbf{T}_{12}^0(t_f)$. In this work, we have only studied the geometry (kinematics) of a 12-DOF biped robot gait. In future work, we plan to generate the optimal gait of the biped robot. For this,we have to use the dynamics, balancing criteria and optimization technique to generate a feasible optimal gait for the biped robot.

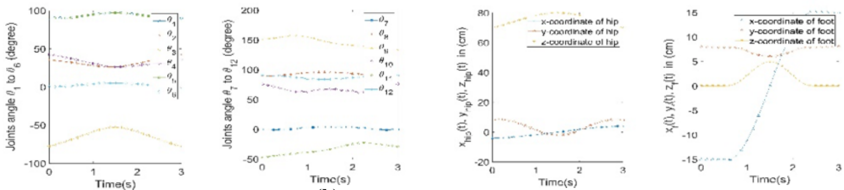

(a) **(b)** **(c)** **(d)**

Figure 4: Biped robot joints angle variation & hip and foot coordinate variation: (a) $\theta_1(t)$ to $\theta_6(t)$, (b) $\theta_7(t)$ to $\theta_{12}(t)$, for $t \in [t_0, t_f]$, (c) x,y,z-coordinates of hip (reference frame-6) , (d) x,y,z-coordinates of foot (reference frame-12).

7. Conclusion

In this paper, we have presented the body trajectory parametrization for generating different types of bipedal gaits. First, we have described forward kinematics, followed by a detailed discussion on inverse kinematics of a 12-DOF biped robot using a geometric method. Then we showed how body trajectory parametrization gives an initial and final homogeneous transformation matrix of hip and foot that can be used to define different types of gaits on uneven terrain. Using the stick diagram, we have demonstrated an example showing the geometry of a bipedal walk on flat ground. In the future, we envision extending this study by including the dynamics of biped robots to obtain an optimally balanced gait by searching for the optimal value of biped robot body trajectory parameters.

Acknowledgement

The authors would like to acknowledge the Design and Simulation Lab of the Mechatronics Department, Center for Advanced Studies Lucknow, for providing the computation facility to complete this research work.

References

[1] J. Kumar and A. Dutta, "Using bilateral symmetry of the biped robot mechanism for efficient and faster optimal gait learning on uneven terrain," *Int. J. Intell. Robot. Appl.*, vol. 5, no. 4, pp. 429–464, 2021.

[2] M. Vukobratović and J. Stepanenko, "On the stability of anthropomorphic systems," *Math. Biosci.*, vol. 15, no. 1–2, pp. 1–37, 1972.

[3] M. Vukobratović and B. Borovac, "Zero-moment point—thirty five years of its life," *Int. J. Humanoid Robot.*, vol. 1, no. 01, pp. 157–173, 2004.

[4] C. Hernández-Santos, E. Rodriguez-Leal, R. Soto, and J. Gordillo, "Kinematics and dynamics of a new 16 DOF humanoid biped robot with active toe joint," *Int. J. Adv. Robot. Syst.*, vol. 9, no. 5, p. 190, 2012.

[5] Q. Huang *et al.*, "Planning walking patterns for a biped robot," *IEEE Trans. Robot. Autom.*, vol. 17, no. 3, pp. 280–289, 2001.

[6] M. Vukobratovic, V. Potkonjak, and S. Tzafestas, "Human and humanoid dynamics," *J. Intell. Robot. Syst.*, vol. 41, no. 1, pp. 65–84, 2004.

[7] C. Chevallereau and Y. Aoustin, "Optimal reference trajectories for walking and running of a biped robot," *Robotica*, vol. 19, no. 5, pp. 557–569, 2001.

[8] G. Dip, V. Prahlad, and P. D. Kien, "Genetic algorithm-based optimal bipedal walking gait synthesis considering tradeoff between stability margin and speed," *Robotica*, vol. 27, no. 3, pp. 355–365, 2009.

[9] D. Tlalolini, C. Chevallereau, and Y. Aoustin, "Comparison of different gaits with rotation of the feet for a planar biped," *Robot. Auton. Syst.*, vol. 57, no. 4, pp. 371–383, 2009.

[10] G. Capi, Y. Nasu, L. Barolli, K. Mitobe, and K. Takeda, "Application of genetic algorithms for biped robot gait synthesis optimization during walking and going up-stairs," *Adv. Robot.*, vol. 15, no. 6, pp. 675–694, 2001.

[11] J. Denavit and R. S. Hartenberg, "A kinematic notation for lower-pair mechanisms based on matrices," 1955.

[12] M. Kumagai and T. Emura, "Sensor-Based Walking of Humanoid Type Biped Robot ina Curve (in Japanese)," 1997, pp. 839–840.

[13] E. Neha, M. Suhaib, and S. Mukherjee, "Motion planning for a four-fingered robotic hand," in *Proceedings of the Advances in Robotics*, 2017, pp. 1–5.

[14] E. Neha, M. Suhaib, S. Mukherjee, and Y. Shrivastava, "Kinematic analysis of four-fingered tendon actuated robotic hand," *Aust. J. Mech. Eng.*, pp. 1–11, 2021.

[15] E. Neha, M. F. Orlando, M. Suhaib, and Y. Shrivastava, "An effort for resolving redundancy of a multi-finger robotic hand in straight-line motions," *J. Braz. Soc. Mech. Sci. Eng.*, vol. 42, no. 11, pp. 1–27, 2020.

[16] E. Rodriguez-Leal, J. S. Dai, and G. R. Pennock, "Kinematic analysis of a 5-R SP parallel mechanism with centralized motion," *Meccanica*, vol. 46, no. 1, pp. 221–237, 2011.

[17] A. Faller and M. Schünke, *The human body: an introduction to structure and function*. Thieme, 2004.